

Generation of the second optical harmonic induced by an electric field in nematic and smectic liquid crystals

M. I. Barnik, L. M. Blinov, A. M. Dorozhkin, and N. M. Shtykov

Scientific Research Institute of Organic Intermediate Products and Dyes
(Submitted 16 June 1981)
Zh. Eksp. Teor. Fiz. **81**, 1763-1770 (November 1981)

Second-harmonic generation induced by an electric field is investigated in the nematic and smectic-A phases of liquid crystals. The temperature dependences of the coherence lengths and of the nonlinear third-order susceptibilities are measured, and the effective hyperpolarizabilities of the second and third orders are calculated. The directions of the phase synchronism and the cubic susceptibilities responsible for the generation of the second harmonic are determined for interactions of the $ee-o$ type.

PACS numbers: 78.20.Jq, 78.20.Dj

1. INTRODUCTION

Investigations of the second-harmonic (SH) generation, induced by a constant electric field are used to determine the hyperpolarizabilities of second (β) and third (γ) orders of molecules of organic substances in the liquid and gaseous phases. These investigations also provide a convenient method of studying the effect of intramolecular and intermolecular interactions on the hyperpolarizability and of obtaining new information about the electronic structure of the molecules.¹⁻⁴

It is of interest to investigate the generation of a SH, induced by an electric field, in liquid crystals, since the value of the cubic nonlinear susceptibility Γ in this case is determined both by the molecular hyperpolarizabilities β_{ijk} and γ_{ijkl} and by the long-range orientational ordering of the molecules in the mesophase. In this connection, measurement of the parameter Γ may serve as a means of investigating the degree of order and the structure of the liquid-crystalline phases. Furthermore, the presence of double refraction in liquid crystals may be used to attain a condition of phase synchronism. The promising character of investigation of nematic liquid crystals by the method of electric-field induced generation of a SH was demonstrated in Refs. 5 and 6.

The present paper is devoted to investigation of nonlinear optical properties of liquid crystals that possess nematic and smectic-A phases. We studied SH generation induced by a constant electric field in *p-n*-octyl-*p'*-cyanobiphenyl (8CB). The choice of the material 8CB was determined by the presence in it of smectic and nematic phases within a temperature range convenient for measurements and by the availability of reliable data on the temperature variations of the index of refraction, the order parameter, and the dielectric constants.

Because nonlinear optical properties of liquid crystals have been little studied, special attention was paid in this work to questions of method. For this purpose, we made measurements also on *p-n*-pentyl-*p'*-cyanoliphenyl (5CB), which had been studied in detail earlier.^{5,6} We measured experimentally the intensity $I_{2\omega}$ of the second harmonic and the coherence length l and their temperature dependence, in the liquid-crystalline

phase ($I_{2\omega}^{\parallel, \perp}, l_{\parallel, \perp}$) and in the isotropic ($I_{2\omega}^{is}, l_{is}$); from these we calculated, respectively, the two characteristic components of the third-order susceptibility, $\Gamma_{xxxx} = \Gamma_{\parallel}$ and $\Gamma_{xxxx} = \Gamma_{\perp}$, and Γ_{is} (here it is supposed that the director of the liquid crystal is oriented along the z axis, and the indices \parallel and \perp correspond to the directions along and transverse to the director, i.e., to the optic axis). From the results of these measurements, we found the effective hyperpolarizabilities of second order, β_3^* , and of third, $\gamma_{\parallel, \perp}^*$.

2. EXPERIMENTAL METHOD

A sketch of the experimental setup for investigation of electric-field induced generation of a second harmonic is shown in Fig. 1. For pumping we used a Q-switched Nd³⁺-YAG pulsed laser LTIPCh-7 (1) with radiation wavelength 1.064 μm , with pulse-repetition frequency 2-125 GHz. The peak power of the pumping pulses was 200-300 kW. At the output of the laser was installed the fundamental-radiation filter (2). The fundamental radiation of the laser was focused on the specimen (6), which was enclosed in a thermostat, by the long-focus lens (3), with $f = 43$ cm. By means of the light-splitting plate (4), a part of the radiation was directed to the photodiode (5) for monitoring of the level of the pumping. Installed past the specimen were the

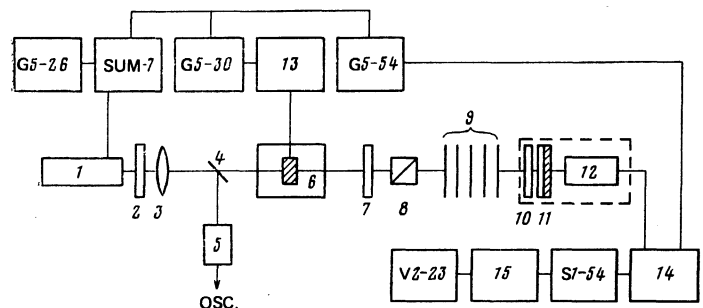


FIG. 1. Sketch of experimental setup: 1, laser; 2, filter for main radiation; 3, long-focus lens; 4, light-splitting plate; 5, vacuum photodiode; 6, temperature-controlled chamber with cell; 7, attenuator for main radiation; 8, analyzer; 9, neutral-density filters; 10, attenuator for fundamental radiation; 11, interference light filter; 12, photomultiplier FEU-79; 13, high-voltage pulse generator; 14, analog switch; 15, integrator.

fundamental-radiation attenuator (7) and the analyzer (8) for control of the polarization of the SH. The SH signal, attenuated by the neutral-density glasses (9) the number of times required in order to bring the recording system into the linear range, fell on the FEU-79 photomultiplier (12). Directly in the housing of the photomultiplier, in front of the photocathode, were placed the SZS-22 glasses (10) for absorption of the pumping radiation and the interference light filter (11) at wavelength 532 nm. The pulsed electric signal from the photomultiplier, through an emitter follower mounted directly within the housing of the photomultiplier, entered the analog switch with preamplifier (14) and then an oscilloscope. The amplified signal from the vertical-deflection plates of the oscilloscope was fed to the integrator (15). The integrated signal is measured with a V2-23 digital voltmeter. Use of the oscilloscope as an amplifier provided a possibility of simultaneously observing the shape of the signal pulse. The laser was triggered by pulses from a G5-26 generator. The delay pulse of a Pockels cell was fed from the control system by the SUM-7 modulator to trigger the G5-30 and G5-54 generators. From the delayed channel of the first generator, a trigger pulse was fed to the high-voltage pulse generator (13). From the delayed channel of the second generator, a strobe pulse of duration 0.7 μ sec, synchronous with the pumping pulse, was fed to the analog switch (14). The purpose of the analog switch was to transmit the signal pulses from the photomultiplier to the subsequent elements of the recording system only at the instant of action of the strobe pulse. The generator (13) produced voltage pulses of duration 20 μ sec and amplitude up to 4 kV, which were fed to the liquid-crystal cell. When the distance between the electrodes was 2 mm, the field on the cell reached 20 kV/cm. The pulse duration was selected on the basis of the condition $\tau < t_p < T$, where τ is the relaxation time of dipole polarization and T is the relaxation time of the director. Some of the experiments on 5CB were carried out at constant electric field with voltage up to 300 V. The temperature of the cell was stabilized with accuracy 0.1 $^{\circ}$ C.

The coherence lengths l_{\parallel} and l_{\perp} and the intensities $I_{2\omega}^{\parallel}$ and $I_{2\omega}^{\perp}$ of the second harmonic at the maxima of the Maker oscillations, which were necessary for calculation of the nonlinear susceptibilities \parallel and \perp , were measured in wedge-shaped cells Fig. 2(a). The values of l_{\parallel} , $I_{2\omega}^{\parallel}$, and Γ_{\parallel} were determined on cells with planar orientation of the liquid crystal at the glass (director oriented along the z axis). Here the directions of the inducing electric field and of the electric fields of the pumping radiation and of the SH were parallel to the director. The measurements of the values of l_{\perp} , $I_{2\omega}^{\perp}$, and Γ_{\perp} were made on cells with homeotropic orientation of the liquid crystal at the glass (director oriented along the y axis), and the directions of all the electric fields were perpendicular to the director (along the z axis). To obtain a planar orientation, the glasses were covered with a film of polyvinyl alcohol of thickness ≈ 500 \AA and were rubbed with fabric. Homeotropic orientation was achieved by coating the glasses with films of chromolan (chromium stearylchloride). Aluminum

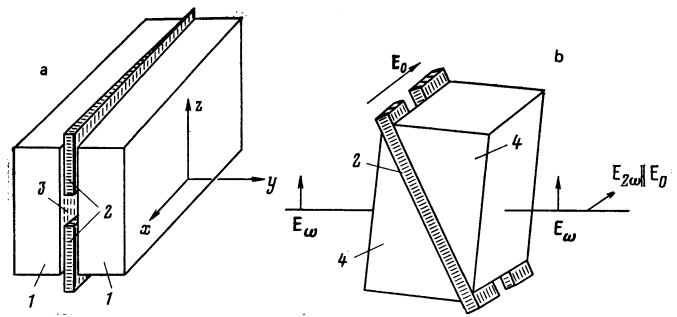


FIG. 2. Configuration of cell of planar type (a) and cell for observation of angular phase synchronism (b): 1, plane-parallel glass plates; 2, electrodes; 3, liquid crystal; 4, 30-degree glass prisms. The y axis is the direction of propagation of the radiation.

foil, of thickness 20 and 50 μ m, was used as electrodes. The quality of the orientation of the liquid crystal was periodically checked with a polarization microscope. The angle of the cell wedge was measured with a G-5 goniometer. The accuracy of measurement of the coherence lengths l_{\parallel} and l_{\perp} was $\leq 3\%$. The absolute values of Γ_{\parallel} and Γ_{\perp} were measured relatively to the component d_{11} of quartz, which was taken as 0.8×10^{-9} cgs esu.

For investigation of the generation of the SH under conditions of phase synchronism, a cell was used that was composed of right-angled prisms, one of the acute angles of which was 30 $^{\circ}$. In this case, the measurements were made on cells with homeotropic orientation of the liquid crystal at the glasses.

3. EXPERIMENTAL RESULTS

In both experimental geometries (all fields parallel or perpendicular to the director), the intensity of the SH was proportional to the square of the intensity E_0 of the inducing electric field and to the square of the power P_{ω} of the pumping radiation. The variation of $I_{2\omega}$ with E_0^2 is shown in Fig. 3 for the cases of constant and of pulsed fields. For pulsed fields, $I_{2\omega}$ varies linearly with E_0^2 over the whole range of measurement of E_0 . But for a constant inducing field, the variation of

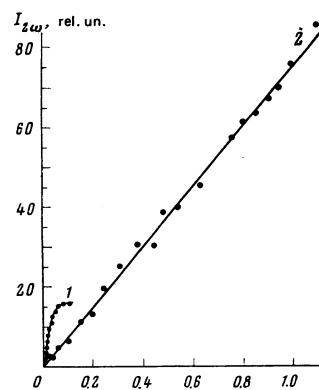


FIG. 3. Variation of intensity of second harmonic $I_{2\omega}$ with square of intensity of inducing field E_0^2 (kV^2/cm^2), for the case of a constant voltage (1) and of a pulsed voltage (2) (5CB, $t = 23^{\circ}$ C).

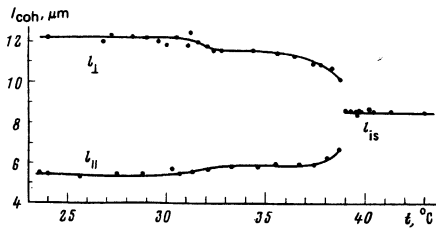


FIG. 4. Variation of coherence lengths with temperature for 8CB.

$I_{2\omega}$ with E_0^2 goes to saturation at voltages on the cell >200 V. By special experiments on observation of the motion of solid particles of foreign impurities, it was established that for voltages ≥ 100 V on the cell, an electrohydrodynamic instability develops in the liquid-crystal layer; this is evidently responsible for the limitation on the increase of $I_{2\omega}$ with increase of E_0 . This is also indicated by the fact that for all pulsed voltages and also for constant voltages up to ~ 100 V, the polarization of the SH was parallel to E_0 , but for constant voltages above 200 V there appears in the SH some radiation with a polarization perpendicular to E_0 , i.e., there actually occurs a depolarization of the SH.

The temperature variations of the coherence lengths for 8CB are shown in Fig. 4. As was shown in Ref. 5, there are the following simple relations between the coherence lengths in the liquid-crystalline ($l_{\parallel, \perp}$) and isotropic (l_{is}) phases:

$$\frac{1}{l_{\parallel}} - \frac{1}{l_{is}} = K \langle P_2 \rangle, \quad \frac{1}{l_{\perp}} - \frac{1}{l_{is}} = \frac{K}{2} \langle P_2 \rangle, \quad (1)$$

where $\langle P_2 \rangle$ is the degree of orientational order. Using the results of the measurements of $l_{\parallel, \perp}$, we calculated the temperature behavior of the order parameter. The constant K was found from the condition that when $t - t_{is} = 17^\circ\text{C}$, the parameter $\langle P_2 \rangle = 0.64$.⁷ The curve obtained is shown in Fig. 5, in which, for comparison, is also shown the temperature dependence of $\langle P_2 \rangle$ obtained from measurements of the index of refraction.⁷ As is seen from the figure, the two methods of determination of $\langle P_2 \rangle$ give results in qualitative agreement.

The coherence lengths for 5CB were measured only in the nematic phase, at room temperature ($t = 25^\circ\text{C}$). As is seen from Table I, the experimental data agree well with a calculation based on the index of refraction.⁶

The experimental temperature variations of the intensities $I_{2\omega}^{\parallel}$ and $I_{2\omega}^{\perp}$ at the maxima of the Maker oscillations, normalized on the value of the intensity $I_{2\omega}^{is}$ of the SH in the isotropic phase, are shown in Fig. 6.

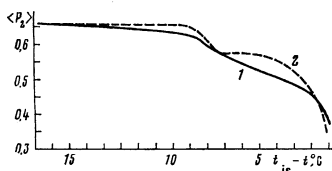


FIG. 5. Temperature variation of the order parameter for 8CB. 1) results of Ref. 7; 2) calculations by formula (1).

TABLE I.

Parameters	5CB		8CB	
	theory	experiment	23° C	33° C
$l_{\parallel}, \mu\text{m}$	4.88	4.80	5.4	5.85
$l_{\perp}, \mu\text{m}$	9.96	9.88	12.2	11.65
$l_{nb}, \mu\text{m}$	—	8.30	—	—
$\Gamma_{\parallel} \cdot 10^{14}, \text{cgs esu}$	—	270	580	630
$\Gamma_{\perp} \cdot 10^{14}, \text{cgs esu}$	—	55	77	112
$\Gamma_c \cdot 10^{14}, \text{cgs esu}$	—	21	21	—
$\Gamma_{nb} \cdot 10^{14}, \text{cgs esu}$	—	167	—	—
θ_c, deg	25.9	26.05	23.5	—
$\gamma_{\parallel}^* \cdot 10^{36}, \text{cgs esu}$	—	126	330	360
$\gamma_{\perp}^* \cdot 10^{36}, \text{cgs esu}$	—	36	63	92
$\gamma_c^* \cdot 10^{36}, \text{cgs esu}$	—	13	15	—
$\gamma_{nb}^* \cdot 10^{36}, \text{cgs esu}$	—	43	—	—
$\beta_{\parallel}^* \cdot 10^{31}, \text{cgs esu}$	—	46	—	126 (39° C)
$\beta_{nb}^* \cdot 10^{31}, \text{cgs esu}$	—	20	—	—

The accuracy of the measurement was 10%. The calculations of the relative nonlinear susceptibilities $R_{\parallel} = \Gamma_{\parallel}/\Gamma_{is}$ and $R_{\perp} = \Gamma_{\perp}/\Gamma_{is}$ were made with the formulas

$$R_{\parallel, \perp} = \frac{(n_{\omega}^{gl} + n_{\omega}^{\parallel, \perp})^2 l_{is}}{(n_{\omega}^{gl} + n_{\omega}^{is})^2 l_{\parallel, \perp}} K_{\parallel, \perp}^{1/2} + \frac{\Gamma_{gl} l_{gl}}{\Gamma_{is} l_{\parallel, \perp}} (1 - K_{\parallel, \perp}^{1/2}), \quad (2)$$

where $K_{\parallel} = I_{2\omega}^{\parallel}/I_{2\omega}^{is}$ and $K_{\perp} = I_{2\omega}^{\perp}/I_{2\omega}^{is}$; n_{ω}^{gl} , l_{gl} , and Γ_{gl} are, respectively, the index of refraction, the coherence length, and the cubic nonlinear susceptibility of glass^{3,4}; n_{ω}^{is} is the index of refraction of the liquid crystal in the isotropic phase. In the derivation of formulas (2), we have neglected the slight temperature dependence of Γ_{gl} , l_{gl} , and n_{ω}^{gl} . The temperature variations of R_{\parallel} and R_{\perp} are shown in Fig. 7.

For 5CB and 8CB at room temperature, we measured the dependence of the intensity of the second harmonic on the angle θ between the direction of the director \mathbf{n} and the wave vector \mathbf{K}_{ω} of the pumping wave, under interaction of the $ee-o$ type Fig. 2(b). The variation of the intensity of the SH with the angle θ in the case of 8CB is shown in Fig. 8, and the angles of phase synchronism θ_c and the corresponding components of the cubic susceptibility Γ_c for both liquid crystals are given in Table I. We note the good agreement of experimental and calculated values of θ_c for 8CB.

4. DISCUSSION OF RESULTS

The third-order nonlinear susceptibilities Γ_{\parallel} and Γ_{\perp} depend on the molecular parameters of the substance and on the degree of orientational order in the mesophase⁵:

$$\Gamma_{\parallel} = N (f_0 f_{\omega}^2 f_{2\omega})_{\parallel} \gamma_{\parallel} = N (f_0 f_{\omega}^2 f_{2\omega})_{\parallel} (\gamma_{is} + 2/\alpha \langle P_2 \rangle + 3/\beta \langle P_4 \rangle), \quad (3)$$

$$\Gamma_{\perp} = N (f_0 f_{\omega}^2 f_{2\omega})_{\perp} \gamma_{\perp} = N (f_0 f_{\omega}^2 f_{2\omega})_{\perp} (\gamma_{is} - 1/\alpha \langle P_2 \rangle + 3/\beta \langle P_4 \rangle). \quad (4)$$

Here N is the number of molecules in unit volume;

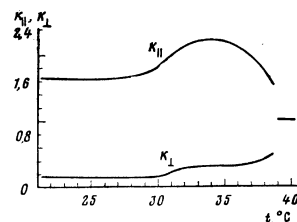


FIG. 6. Temperature variation of the intensity of the second harmonic for 8CB.

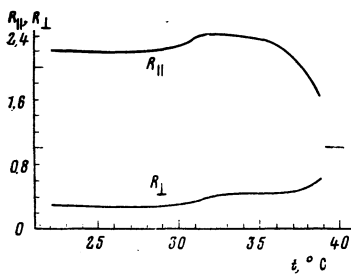


FIG. 7. Temperature variation of the cubic nonlinear susceptibility for 8CB. Absolute value of $\Gamma_{\text{is}} = 265 \cdot 10^{-14}$ cgs esu.

$(f_0 f_{\omega}^2 f_{2\omega})_{\parallel}$ and $(f_0 f_{\omega}^2 f_{2\omega})_{\perp}$ are local-field factors in the mesophase for directions respectively along and transverse to the director at the frequencies of the inducing field (f_0), of the field of the main radiation (f_{ω}), and of the field of the second harmonic ($f_{2\omega}$); γ_{\parallel} and γ_{\perp} are the total molecular hyperpolarizabilities of the third order along and transverse to the long axes of the molecules; γ_{is} is the total hyperpolarizability for an isotropic orientational distribution function of the molecules; α and β are the contributions to the nonlinear susceptibility per molecule due to the presence of orientational order of the liquid crystal; and $\langle P_2 \rangle$ and $\langle P_4 \rangle$ are coefficients of the expansion of the orientational distribution function of the molecular axes with respect to the direction of the director.

According to formulas (3) and (4), the total third-order hyperpolarizabilities γ_{\parallel} and γ_{\perp} can be calculated if the local-field factors are known. The effective hyperpolarizabilities γ_{\parallel}^* and γ_{\perp}^* obtained in the approximation of an isotropic local-field factor, in Vuks form, are given in Table I. Also given there are the effective second-order hyperpolarizabilities $\beta_3^* = \beta_{333} + \beta_{322} + \beta_{311}$. For comparison, the table gives also the nonlinear susceptibility Γ_{nb} , the hyperpolarizabilities γ_{nb} and β_{nb} , and the coherence length l_{nb} of nitrobenzene according to the data of Ref. 4.

Since $\beta \ll \alpha$ and $\langle P_4 \rangle < \langle P_2 \rangle$, the third terms in parentheses in equations (3) and (4) are negligibly small in comparison with the first two. By neglecting also the slight temperature dependence of N and introducing the notation $(f_0 f_{\omega}^2 f_{2\omega})_{\parallel} = F_{\parallel}$ and $(f_0 f_{\omega}^2 f_{2\omega})_{\perp} = F_{\perp}$, we reduce equations (3) and (4) to the form

$$R_{\parallel} = \frac{\Gamma_{\parallel}}{\Gamma_{\text{is}}} = \frac{F_{\parallel}}{F_{\text{is}}} \left(\frac{T_{\text{is}}}{T} + \frac{2}{7} \frac{\alpha}{\gamma_{\text{is}}} \langle P_2 \rangle \right), \quad (5)$$

$$R_{\perp} = \frac{\Gamma_{\perp}}{\Gamma_{\text{is}}} = \frac{F_{\perp}}{F_{\text{is}}} \left(\frac{T_{\text{is}}}{T} - \frac{1}{7} \frac{\alpha}{\gamma_{\text{is}}} \langle P_2 \rangle \right), \quad (6)$$

If we suppose that $F_{\parallel} = F_{\perp} = F_{\text{is}}$, then it is easily seen that, for example, formula (5) gets into contradiction with experiment for 8CB. In fact, it follows from formula (5) that on transition from the nematic to the smectic phase, the nonlinear susceptibility Γ_{\parallel} should increase because of increase of the degree of ordering $\langle P_2 \rangle$ (see Fig. 5). But experimentally, a decrease of

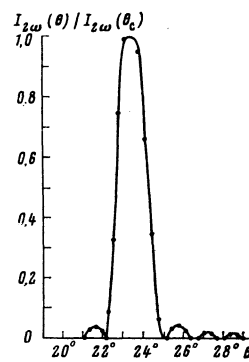


FIG. 8. Variation of the intensity of the second harmonic $I_{2\omega}$ with the angle θ between the director and the wave vector of the primary wave, for 8CB ($t = 23^\circ\text{C}$).

the parameter Γ_{\parallel} is observed at the phase-transition point (see Fig. 7).

The dielectric constant ϵ_{\parallel} of the compound 8CB undergoes a similar anomaly of the temperature behavior.⁸ In this case, a decrease of ϵ_{\parallel} is caused by the increase of antiparallel correlation of dipoles in the smectic phase.⁹ This leads to a decrease of the effective dipole moment μ^* per molecule. Consequently the decrease of Γ_{\parallel} can be attributed to a decrease of the parameter α , which is a combination of the constant dipole moment μ of the molecule and its second-order hyperpolarizability $\beta_{ij,k}$. It is possible that the reorganization of the spatial molecular structure of the liquid crystal on transition from the nematic to the smectic phase and the enhancement of the antiparallel correlation of the dipoles exert an influence also on the second-order hyperpolarizability. And in fact the decrease of Γ_{\parallel} cannot be described quantitatively solely on the basis of the decrease of the dipole moment μ^* , calculated from the temperature variation of ϵ_{\parallel} .

In conclusion, we note that an alternative explanation of the decrease of Γ_{\parallel} , which was described above in the language of effective parameters μ^* and β^* , can apparently be given in terms of a change of the local-field factors on transition from the nematic to the smectic phase.

¹J. F. Ward and I. J. Bigio, Phys. Rev. **A11**, 60 (1975).

²C. G. Bethea, J. Chem. Phys. **69**, 1312 (1978).

³J. L. Oudar, J. Chem. Phys. **67**, 446 (1977).

⁴B. F. Levine and C. G. Bethea, J. Chem. Phys. **63**, 2666 (1975).

⁵S. K. Saha and G. K. Wong, Appl. Phys. Lett. **34**, 423 (1979).

⁶S. K. Saha and G. K. Wong, Opt. Commun. **30**, 119 (1979).

⁷R. G. Horn, J. Phys. (Paris) **39**, 105 (1978).

⁸C. Druon and J. M. Wacrenier, J. Phys. (Paris) **38**, 47 (1977).

⁹W. H. De Jeu, W. J. A. Goossens, and P. Bordewijk, J. Chem. Phys. **61**, 1985 (1974).

Translated by W. F. Brown, Jr.